Accepted Manuscript

A structure-guided optimization of pyrido[2,3-*d*]pyrimidin-7-ones as selective inhibitors of $EGFR^{L858R/T790M}$ mutant with improved pharmacokinetic properties

Lei Yu, Minhao Huang, Tianfeng Xu, Linjiang Tong, Xiao-e Yan, Zhang Zhang, Yong Xu, Caihong Yun, Hua Xie, Ke Ding, Xiaoyun Lu

PII: S0223-5234(16)31012-1

DOI: 10.1016/j.ejmech.2016.12.006

Reference: EJMECH 9097

To appear in: *European Journal of Medicinal Chemistry*

Received Date: 30 September 2016

Revised Date: 24 November 2016

Accepted Date: 2 December 2016

Please cite this article as: L. Yu, M. Huang, T. Xu, L. Tong, X.-e Yan, Z. Zhang, Y. Xu, C. Yun, H. Xie, K. Ding, X. Lu, A structure-guided optimization of pyrido[2,3-*d*]pyrimidin-7-ones as selective inhibitors of $EGFR^{L858R/T790M}$ mutant with improved pharmacokinetic properties, *European Journal of Medicinal Chemistry* (2017), doi: 10.1016/j.ejmech.2016.12.006.

A Structure-Guided Optimization of Pyrido[2,3-*d*]pyrimidin-7-ones as Selective Inhibitors of EGFR$^{L858R/T790M}$ Mutant with Improved Pharmacokinetic Properties

Lei Yu[a,b], Minhao Huang[a,b], Tianfeng Xu[a,b], Linjiang Tong[d], Xiao-e Yan[e], Zhang Zhang[a], Yong Xu[a], Caihong Yun[e], Hua Xie[d]*, Ke Ding[a,c]*, Xiaoyun Lu[c]*

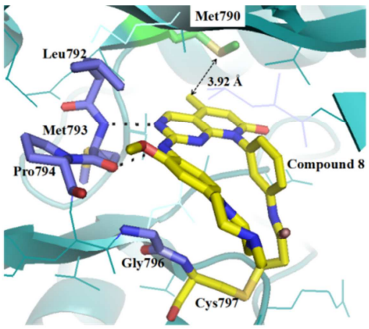

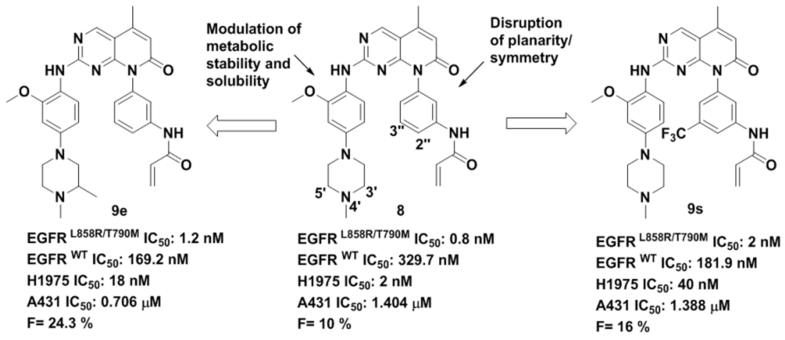

Structural optimization of pyrido[2,3-*d*]pyrimidin-7-ones yielded new selective EGFR^{T790M} inhibitors. Compound **9s** exhibited good pharmacokinetic properties with F value of 16%, and inhibited EGFR$^{L858R/T790M}$ kinase and H1975 cells with IC_{50} values of 2.0 and 40 nM, respectively.

A Structure-Guided Optimization of Pyrido[2,3-*d*]pyrimidin-7-ones as Selective Inhibitors of EGFR$^{L858R/T790M}$ Mutant with Improved Pharmacokinetic Properties

Lei Yu[a,b], Minhao Huang[a,b], Tianfeng Xu[a,b], Linjiang Tong[d], Xiao-e Yan[e], Zhang Zhang[a], Yong Xu[a], Caihong Yun[e], Hua Xie[d]*, Ke Ding[a,c]*, Xiaoyun Lu[c]*

[a] Guangzhou Institutes of Biomedicine and Health, Chinese Academy of Sciences, No. 190 Kaiyuan Avenue, Guangzhou 510530, China

[b] University of Chinese Academy of Sciences, No. 19 Yuquan Road, Beijing 100049, China

[c] School of pharmacy, Jinan University, No. 601 Huangpu Avenue West, Guangzhou 510632, China.

[d] State Key Laboratory of Drug Research, Shanghai Institute of Materia Medica, Chinese Academy of Sciences, No. 555 Zu-Chong-Zhi Road, Zhangjiang Hi-Tech Park, Shanghai 201203, China

[e] Peking University Institute of Systems Biomedicine and Department of Biophysics, Peking University Health Science Center, Beijing 100191, China

Corresponding authors: Tel: +86-20-85221523. E-mail: ding_ke@gibh.ac.cn; luxy2016@jnu.edu.cn.

Abstract

Structural optimization of pyrido[2,3-*d*]pyrimidin-7-ones was conducted to yield a series of new selective EGFR^{T790M} inhibitors with improved pharmacokinetic properties. One of the most promising compound **9s** potently suppressed EGFR$^{L858R/T790M}$ kinase and inhibited the proliferation of H1975 cells with IC_{50} values of 2.0 nM and 40 nM, respectively. The compound dose-dependently induced reduction of the phosphorylation of EGFR and downstream activation of ERK in NCI-H1975 cells. It also exhibited moderate plasma exposure after oral administration and an oral bioavailability value of 16 %. Compound **9s** may serve as a promising lead compound for further drug discovery overcoming the acquired resistance of non-small cell lung cancer (NSCLC) patients.

Keyword: EGFR^{T790M} mutant, Pyrido[2,3-*d*]pyrimidin-7-ones, Pharmacokinetic property, NSCLC, Irreversible inhibitor

1. Introduction

The epidermal growth factor receptor (EGFR, ErbB1, HER1) is a well-validated molecular target for drug discovery treating non-small-cell lung cancer (NSCLC) patients [1]. Several small molecule EGFR inhibitors (e.g., the reversible inhibitors gefitinib [2], erlotinib [3] and irreversible inhibitor afatinib [4] etc.) have achieved significant clinical benefits in NSCLC patients with active mutations in EGFR tyrosine kinase domain (i.e. L858R mutation in exon 21 and del E746-A750 mutation in exon 19) [5]. However, acquired resistance against the current inhibitors becomes a major challenge for clinical management of NSCLC patients [6]. A secondary threonine^{790} to methionine^{790} mutation is a primary mechanism of the resistance accounting for approximate 50 % resistant NSCLC patients. The 2nd generation irreversible cysteine797-reacting inhibitors have been developed to potentially overcome the EGFR^{T790M} mutation-mediated resistance. Nevertheless, most of them suffer from low clinical maximum tolerated dose (MTD) in resistance patients due to their poor margin over wild-type (WT) EGFR inhibition. To address the "on-target" toxicity, several third- generation EGFR^{T790M} mutant selective inhibitors [7- 11] (e.g., WZ4002 (**1**) [7], rociletinib (**2**) [8], osimertinib (AZD9291) (**3**) [9], olmutinib (**4**) [10] (Fig. **1**)) were developed. These compounds effectively inhibit resistant EGFR^{T790M} mutant while are obvious less potent to EGFR^{WT}. Significantly, the U.S. FDA recently granted an accelerated approval for osimertinib to treat EGFR^{T790M} mutated patients whose disease has gotten worse after treatment of EGFR-blocking therapy [9b].

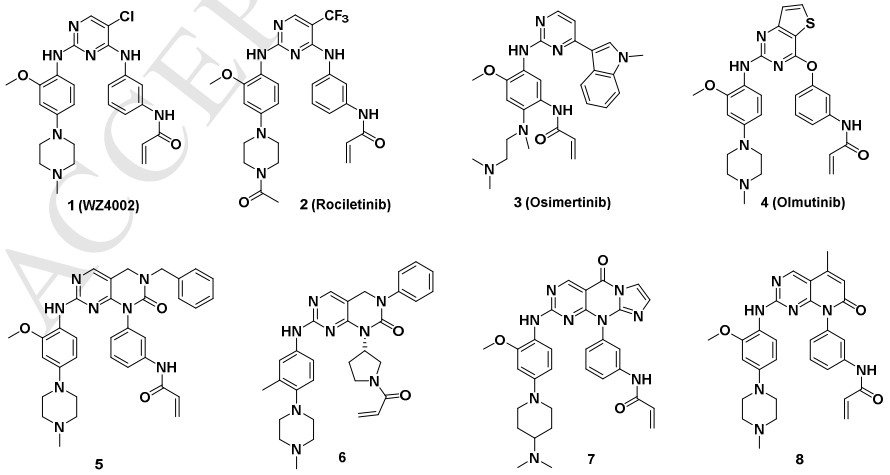

Figure 1. Chemical structures of newly reported selective irreversible EGFR^{T790M} inhibitors.

Our group had explored great efforts to discover novel EGFR^{T790M} mutant selective inhibitors (Fig. **1**) with distinct chemical scaffolds, such as dihydropyrimido[4,5-*d*]pyrimidinyl (**5** and **6**)

[12], pyrimidine [4,5-*d*]pyrimidin-4(1*H*)-one (**7**) [13], and pyrido[2,3-*d*]pyrimidine-7-one derivatives (**8**) [14]. The compound **8** displayed highly potent and specific $EGFR^{T790M}$ inhibition ($EGFR^{L858R/T790M}$ IC_{50} = 0.8 nM) and strongly suppressed the proliferation of $EGFR^{T790M}$ mutated H1975 NSCLC cells with an IC_{50} value of 2.8 nM. However, it possesses unacceptable pharmacokinetic (PK) parameters such as poor oral bioavailability (F = 10 %), low oral exposure and rapid clearance which limit the further development. Herein, we describe further structural optimization of the compound with an aim of improving its PK profiles.

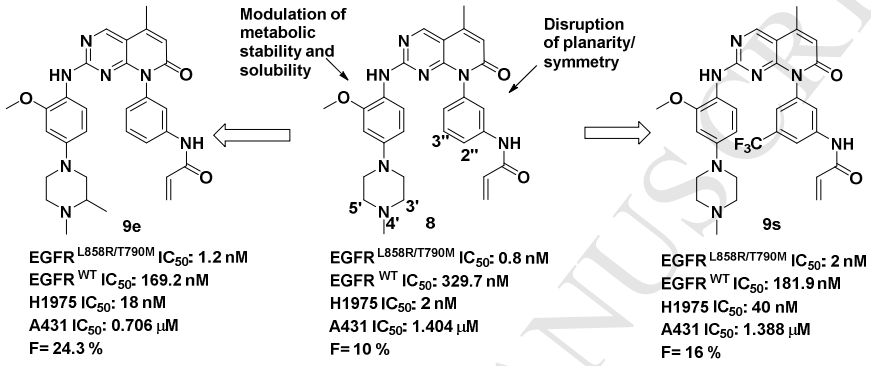

Figure 2. Pharmacokinetic property-based modification of the pyrido[2,3-*d*]pyrimidine-7-ones as selective $EGFR^{T790M}$ inhibitors

2. Chemistry

Syntheses of the designed compounds **9a**- **9u** is outlined in Scheme **1**. A directly nucleophilic coupling of commercially available 5-bromo-2, 4-dichloropyrimidine (**10**) with *N*-Boc amine (**11**) produced intermediates **12**. Compounds **12** were then reacted with trans-but-2-enoic acid under Heck coupling conditions [14] in the presence of bis(benzonitrile)palladium(II) dichloride, followed by a treatment with acetic anhydride to produce the key intermediates **13**. The intermediates **13** were coupled with various amines (**14**) and followed by deprotection to yield substituted amines **15**. Compounds **9a**- **9u** were finally obtained by a straightforward acryloylation of **15**.

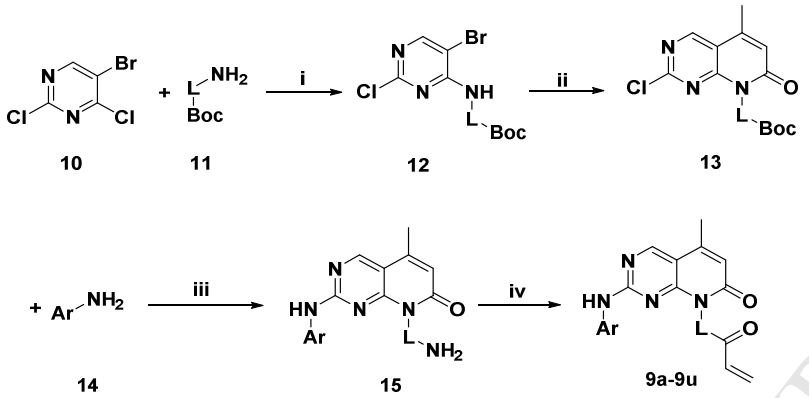

Scheme 1. Synthesis of compounds **9a- 9u**. Reagents and conditions: (i) K_2CO_3, *N*, *N*-dimethylformamide, 80- 95 %, (ii) a. (*E*)-but-2-enoic acid, bis(benzonitrile)palladium(II) dichloride, tri(*o*-tolyl)phosphine, *N*, *N*-diisopropylethylamine, tetrahydrofuran, 70 °C, argon, 16 hrs, b. Acetic anhydride, 90 °C, 24 hrs, 25- 50 %, (iii) a. for **9d**, K_3PO_4, tris(dibenzylideneacetone)dipalladium(0), 2-(dicyclohexylphosphino)-2',4',6'-triisopropylbiphenyl, 110 °C; for **9a** to **9u**, 2-butanol, trifluoroacetic acid, 90- 110 °C, 18 hrs, b. dichloromethane, trifluoroacetic acid, room temperature, 50- 85 % (two steps), (iv) Acrylyl chloride, *N*, *N*-diisopropylethylamine, dichloromethane, 0 °C, 40- 80 %.

3. Results and Discussion

Structural feature analysis of **8** revealed that it adopts a highly planar configuration, which is believed to contribute to the poor solubility and unacceptable pharmacokinetic parameters. Our previous studies have demonstrated that the 5-methyl pyrido[2,3-*d*]pyrimidin-7-one scaffold and the acrylamide moiety are critical for the selective EGFR kinase inhibition [14]. In order to get insight understanding on the binding mode of compound **8** with $EGFR^{T790M}$, a co-crystal structure of the inhibitor complexed with $EGFR^{T790M}$ was determined with a resolution of 2.8 Å (Fig. **3** and SI Table **1**). It was shown that the inhibitor **8** bound to the ATP binding site of EGFR with a "U-shaped" configuration. The pyrido[2,3-*d*]pyrimidine-7-one core formed a bidentate hydrogen bonding interaction with the "hinge" residue Met793 of the protein (Fig. **3A**). The methoxyl substituent of aniline ring extended towards Leu792 and Pro794 in the hinge region and the aniline ring formed a hydrophobic interaction with the α-carbon of Gly796. The 5-methyl group was slipped into the "gatekeeper" residue Met790 which likely contributed to the selectivity of $EGFR^{T790M}$ over the wild-type EGFR (Fig. **3A**) [14].

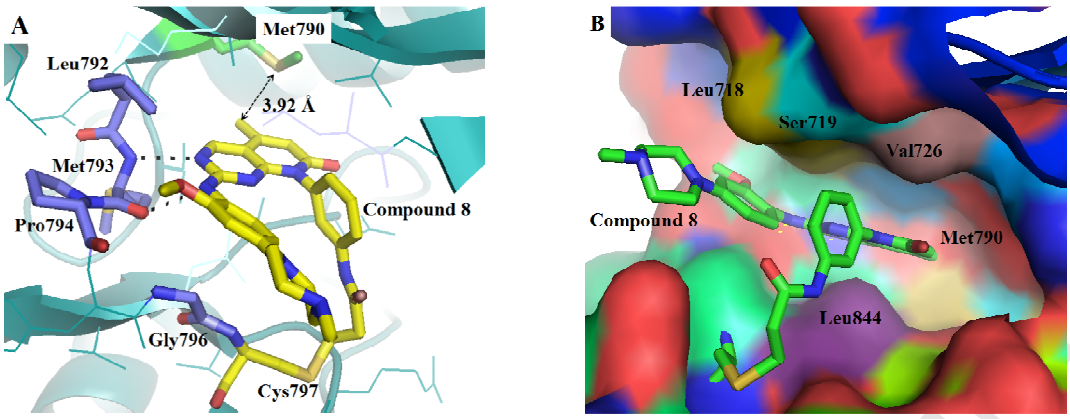

Figure 3. A X-ray crystal structure of compound **8** binding with EGFR^{T790M} (PDB ID: 5GMP). (A) The EGFR^{T790M} kinase is shown in a blue ribbon representation. Compound **8** is shown in yellow stick structure. Hydrogen bonds are indicated by black hatched lines to key amino acids. (B) The X-ray crystal structure with interaction surface is shown.

The X-ray structure analysis also revealed that the left-arm hydrophilic phenylpiperazine moiety of compound **8** was exposed to a solvent accessible surface (Fig. **3B**). It might provide an ideal position for further structural optimization to improve PK profiles of the molecules without affecting the selective EGFR^{T790M} suppression. Thus, compounds **9a** and **9b** which harbored hydrophilic pyrazole substituents were first designed and evaluated to display strong EGFR$^{L858R/T790M}$ inhibition with IC_{50} values of 4.2 and 1.8 nM, respectively (Table **1**). Whereas, both compounds also exhibited significantly less potencies against EGFR^{WT} with IC_{50} values of 444.7 and 166.2 nM, respectively. Pyridine containing compound **9c** and thiazole substituted molecule **9d** were also designed and evaluated to exhibit strong and wild-type sparing EGFR$^{L858R/T790M}$ inhibition with IC_{50} values of 1.4 and 2.5 nM, respectively. In addition, compounds **9c** and **9d** strongly suppressed the proliferation of EGFR^{T790M} mutated H1975 NSCLC cells with IC_{50} values of 64 and 8.0 nM, respectively, while their activities against A431 cells with wild-type EGFR are significantly less potent. Demethylation of the *N*-methyl phenylpiperazine moiety is a possible mechanism contributing to the metabolic liability of compound **8** [15]. Consequently, 3', 4'- dimethylpiperazine (**9e**) and 3', 4', 5'- trimethylpiperazine (**9f**) analogues were synthesized to block the potential *in vivo* demethylation by increasing steric hindrance. Not surprisingly, both **9e** and **9f** exhibited comparable EGFR$^{L858R/T790M}$ inhibitory potencies to that of lead molecule **8** (Table **1**).

Table 1 *In vitro* EGFR inhibition and anti-proliferation data of compounds **9a- 9f.**

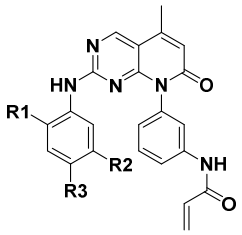

Compds	R_1	R_2	Kinase inhibition[a] (IC_{50}, nM)		Anti-proliferation[b] (IC_{50}, μM)	
			$EGFR^{WT}$	$EGFR^{L858R/T790M}$	H1975[c]	A431[d]
2[e]	-		344.3	4.3	0.042	1.545
3[e]	-		260.4	3.4	0.030	1.604
8	OMe	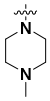	329.7	0.8	0.002	1.404
9a			444.7	4.2	0.289	4.004
9b		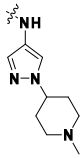	166.2	1.8	0.014	3.525
9c		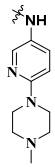	46.8	1.4	0.064	2.379
9d		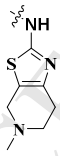	549.6	2.5	0.008	2.698
9e	OMe		169.2	1.2	0.018	0.706
9f	OMe		97.0	3.3	0.004	1.670

[a] EGFR activity assays were performed using an ELISA assay according to the reported protocols [4]. The compounds were incubated with the kinase reaction mixture for 1.0 h before measurement. The data are mean values from 3 independent experiments. [b] The anti-proliferative activities of the compounds were evaluated using the SRB (sulforhodamine B) assay. The data

were means from at least three independent experiments. [c] H1975 is a human lung cancer cell line ($EGFR^{L858R/T790M}$). [d] A431 is an epidermoid carcinoma cell line ($EGFR^{WT}$). [e] These two compounds were synthesized in our laboratory [8, 9].

The X-ray structural information further revealed that the right-arm phenyl ring in compound **8** functioned as a linker between the 5-methyl pyrido[2,3-*d*]pyrimidin-7-one core and an acrylamide to react with Cys797 residue in EGFR protein (Figure. **3B**). Our previous investigations had demonstrated that a replacement of the phenyl ring with a more flexible aliphatic ring is an effective strategy to improve aqueous solubility of the molecules [12b]. Thus, we first replaced the phenyl ring with a flexible 3-methylene-pyrrolidinyl (**9g**) (Table **2**). However, the resulting compound **9g** demonstrated a significant potency loss in both $EGFR^{L858R/T790M}$ kinase (IC_{50} = 63.8 nM) and H1975 cell growth inhibitory (IC_{50} = 305 nM) assays. Several other flexible linkers, such as (*S*)-3-pyrrolidinyl (**9h**), (*R*)-3-pyrrolidinyl (**9i**) and 4-piperidinyl (**9j**) were also explored. Disappointingly, all of these modification caused obvious potency decrease. It was also noteworthy that the *S*-enantiomer **9h** (IC_{50} = 91.8 nM) displayed 5 times better $EGFR^{L858R/T790M}$ inhibitory potency than the corresponding *R*-enantiomer **9i** (IC_{50} = 436 nM), when a 3-pyrrolidinyl moiety was utilized as the linker. Nevertheless, both of the compounds were significantly less potent to suppress the proliferation of H1975 cells harboring EGFR $^{L858R/T790M}$ mutant than the lead molecule **8**.

Table 2 *In vitro* EGFR inhibition and anti-proliferation data of compounds **9g- 9u**

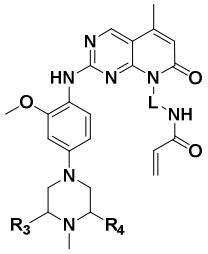

Compds	R_3	R_4	L	Kinase inhibition[a] (IC_{50}, nM)		Anti-proliferation[b] (IC_{50}, μM)	
				$EGFR^{WT}$	$EGFR^{L858R/T790M}$	H1975[c]	A431[d]
2[e]		-		344.3	4.3	0.042	1.545
3[e]		-		260.4	3.4	0.030	1.604

8	H	H		329.7	0.8	0.002	1.404
9g	H	H	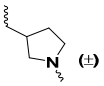	>1000	63.8	0.305	>10
9h	H	H		>1000	91.8	0.762	>10.0
9i	H	H		>1000	436.3	5.200	>10.0
9j	H	H		>1000	>1000	2.235	>10.0
9k	H	H		36.9	2.3	0.081	3.622
9l	H	H		208.4	1.8	0.006	3.248
9m	H	H		472.1	3.4	0.142	1.054
9n	H	H		24.0	2.4	0.120	1.443
9o	H	H		>1000	17.7	0.197	0.660
9p	H	H		26	0.8	0.0001	0.817
9q	H	H		33.1	0.6	0.007	1.428
9r	H	H		57.0	1.8	0.004	1.154
9s	H	H		181.9	2.0	0.040	1.388
9t	H	Me		66.0	1.6	0.012	1.712
9u	Me	Me		97.0	3.3	0.030	1.134

[a] EGFR activity assays were performed using an ELISA assay according to the reported protocols [4]. The compounds were incubated with the kinase reaction mixture for 1.0 h before measurement. The data are mean values from 3 independent experiments. [b] The anti-proliferative activities of the compounds were evaluated using the SRB (sulforhodamine B) assay. The data were means from at least three independent experiments. [c] H1975 is a human lung cancer cell line ($EGFR^{L858R/T790M}$). [d] A431 is an epidermoid carcinoma cell line ($EGFR^{WT}$). [e] These two

compounds were synthesized in our laboratory [8, 9].

Given the fact that a flexible linker is detrimental to $EGFR^{L858R/T790M}$ inhibition, a different optimization strategy is needed to improve pharmacokinetic properties of the molecules. X-ray structure analysis suggested that the right-arm phenyl ring in **8** was accommodated in a partially opened hydrophobic pocket formed by Leu718, Ser719, V726 and Leu844 residues (Fig. **3B**). The 2”- or 3”- positions of the phenyl group might be used to introduce an extra substituent to improve PK parameters by disrupting the molecular planarity and symmetry [16] without obviously affecting $EGFR^{L858R/T790M}$ inhibitory potency. Based on this hypothesis, 2”- methyl (**9k**) and 3”- methyl (**9l**) derivatives were first designed and synthesized. The compounds indeed exhibited strong $EGFR^{L858R/T790M}$ inhibitory activities with IC_{50} values of 2.3 and 1.8 nM, respectively, which is similar to that of **8**. Further analysis also revealed that 3”- methyl compound (**9l**) displayed obviously greater target selectivity than the corresponding 2”- methyl analogue (**9k**) with a factor of 115- fold (Table **2**). Thus, 3”- position of the phenyl group might be an optimal position for introducing substituents to maintain high $EGFR^{L858R/T790M}$ potency and selectivity. Further investigation suggested that 3”- position was well tolerated to several other hydrophobic substituents, such as ethyl (**9m**), isopropyl (**9n**), *tert*-butyl (**9o**), fluoro (**9p**), chloro (**9q**), bromo (**9r**) and trifluoromethyl (**9s**) moieties to keep the strong $EGFR^{L858R/T790M}$ inhibition. Compounds **9m**, **9n**, **9p**, **9q**, and **9r** exhibited comparable $EGFR^{L858R/T790M}$ inhibitory potencies to the lead molecule **8**. These compounds also displayed strong anti-proliferative activities against H1975 NSCLC cells with $EGFR^{L858R/T790M}$ mutation. However, the significantly decreased target specificity of these molecules (comparing with **8**) might limit their potential for further development. It was also noteworthy that the introduction of a tert-butyl group (**9o**) in 3”- position caused a 20-fold potency loss with IC_{50} value of 17.7 nM (Table **2**). This might be due to the steric conflict between bulky group and the hydrophobic residues (Leu718 and Ser719) in the protein. Encouragingly, when a trifluoromethyl group was introduced to the 3”- position, the resulting compound **9s** exhibited comparable $EGFR^{L858R/T790M}$ inhibitory potency to that of **8** with an IC_{50} of 2.0 nM, and also strong anti-proliferative activity with an IC_{50} of 40 nM. This molecule also displayed an approximate 90-fold $EGFR^{L858R/T790M}$ selectivity over $EGFR^{WT}$ (Table **2**). The 3’, 4’-dimethyl (**9t**) and 3’, 4’, 5’-trimethyl (**9u**) derivatives based on **9s** also demonstrated strong $EGFR^{L858R/T790M}$ inhibition and promising target specificity.

Pharmacokinetic parameters of the most potent and selective molecules (i.e. **9d**, **9e, 9f, 9s, 9t** and **9u**) were further determined in male Sprage-Dawley rats (Table **3**). It was shown that compound **9d** displayed poor bioavailability (F = 0.6 %, Table **3**), suggesting the left-arm heterocyclic replacements didn't meet our initial goal for PK parameter improvement. Compounds **9e** and **9f** displayed improved PK properties with bioavailability values of 24.3 % and 13.3 %, respectively. The maximum plasma concentration (C_{max}) and oral exposure (AUC) of compound **9e** were 154.7 μg/ L and 526.4 μg/ L*h, respectively, while the corresponding values of compound **9f** were 64.43 μg/ L and 612.72 μg/ L*h after a single oral administration at 25 mg/kg (Table **3**). Compound **9s** also exhibited improved pharmacokinetics parameters with an oral bioavailability of 16 %, a C_{max} value of 160.7 μg/ L and an AUC value of 670.9 μg/ L*h after an oral dosing of 25 mg/ kg. In addition, compound **9s** demonstrated relatively lower clearance rate (CLz = 6.0 L/ h/Kg) than that of compound **8**. These data collectively suggested that an introduction of trifluoromethyl group at 3''- position of phenyl ring might benefit the PK profile improvement. However, there is no much advantage achieved by combination of the structural elements from **9s** and **9e** or **9f** with that from **9s**. The resulting compounds **9t** and **9u** displayed significantly lower C_{max} and AUC values after oral administration at same dosages (Table **3**).

Table 3. Sprague-Dawley rat PK parameters by intravenous and oral administration[a]

Compds	route	AUC(0→∞) (μg/L*h)	C_{max}(μg/L)	T_{max}(h)	CLz(L/h/Kg)	F(%)
8[b]	iv	450.2	1366.3		11.4	10.8
	po	243.2	83.1	1.563		
9d[c]	iv	887.9	1910		5.7	0.6
	po	26.6	10.6	0.25		
9e[b]	iv	432.7	1334.2		11.8	24.3
	po	526.4	154.7	1.667		
9f[d]	iv	622.21	772.27		8.12	13.33
	po	612.72	64.43	4.00		
9s[b]	iv	831.2	2455		6.1	16.1
	po	670.9	160.7	2		
9t[d]	iv	398.48	259.17		2.25	5.58

	po	111.22	21.36	1.67		
9u[d]	iv	409.65	592.08		12.29	4.38
	po	89.66	17.45	6		

[a] The pharmacokinetic parameters were determined after a single oral administration (25 mg/ kg, n = 3 rats) and intravenous injection (5 mg/ kg, n = 3 rats). [b] Compounds formulated in 2 % dimethyl sulfoxide, 4 % ethanol, 4 % castor oil, and 90 % H_2O. They were treated as a mesylate salt. [c] Compounds formulated in 5 % ethanol, 3 % tween-80 and 92 % H_2O and were treated as a mesylate salt. [d] Compounds were dissolved in 5 % dimethyl sulfoxide, 40 % PEG400 and saline. They were treated as a mesylate salt.

The kinase inhibition of the compound **9s** was further validated by investigating its suppressive functions on the activation of EGFR and the downstream signaling proteins in H1975 NSCLC cells harboring $EGFR^{L858R/T790M}$ mutant. As shown in Figure **4**, compound **9s** caused a dose-dependent reduction of the phosphorylation of EGFR and downstream ERK in H1975 cells. However, it was significantly less potent in A431 cells harboring $EGFR^{WT}$. Thus, compound **9s** displayed selective suppression of phos-EGFR in H1975 cells, which was consistent with our previous investigation [14].

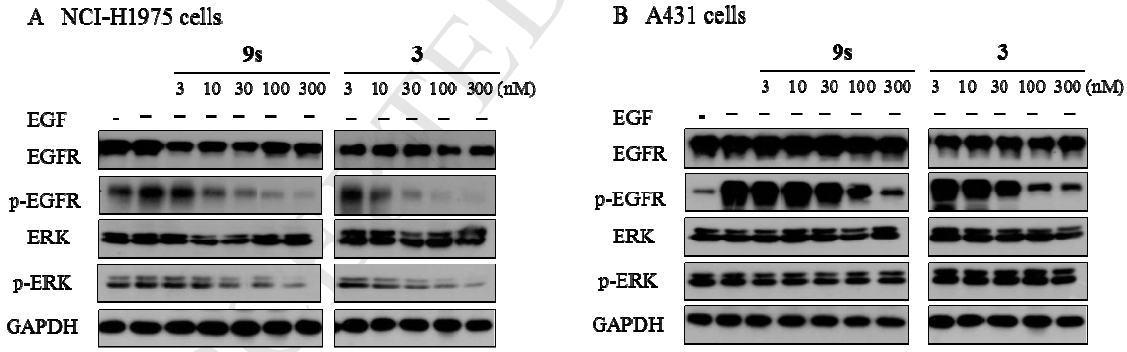

Figure. 4 Compound **9s** potently and selectively inhibits the activation of EGFR signals in H1975 NSCLC cells (A), while less potent in A431 cancer cells (B). Cells were treated with or without compound **9s** and **3** for 4 hrs at indicated concentration, respectively. Cells were then stimulated by 100 ng/ mL EGFR for 10 min and harvested for Western blot analysis.

4. Conclusion

Based on structural feature analysis of $EGFR^{T790M}$ complex with compound **8**, structural optimization of pyrido[2,3-*d*]pyrimidin-7-ones were conducted with an aim to improve the pharmacokinetics profiles of the new irreversible wild-type sparing $EGFR^{L858R/T790M}$ inhibitors.

One of the most promising compound **9s** exhibited moderate pharmacokinetic properties with an oral bioavailability value of 16 %, strong $EGFR^{L858R/T790M}$ inhibitory potency with an IC_{50} of 2.0 nM and promising anti-proliferative activity against gefitinib-resistant H1975 human NSCLC cells with an IC_{50} of 40 nM. The further structural optimization and *in vivo* antitumor efficacy of this compound in different models are undergoing and the results will be disclosed in due course.

5. Experimental Section

5.1 General methods for chemistry

All reagents and solvents used as were purchased from commercial sources without further purification. Flash chromatography was performed using silica gel (200- 300 mesh). All reactions were monitored by TLC, using silica gel plates with fluorescence F_{254} and UV light visualization. ^{1}H NMR and ^{13}C NMR spectra were recorded on a Brucker AV- 400 spectrometer at 400 MHz and Brucker AV- 500 spectrometer at 125 MHz using deuterated solvents as internal standard. Coupling constants (*J*) are expressed in hertz (Hz). Chemical shifts (δ) are given in parts per million (ppm). High resolution ESI- MS were recorded on an Applied Biosystems Q-STAR Elite ESI- LC- MS/ MS mass spectrometer. The purity of compounds was determined with reverse-phase HPLC analysis to be over 95 % (see supporting information). HPLC instrument: Dionex Summit HPLC (Column: Diamonsil C18, 5.0 μm, 4.6 × 250 mm (Agilent Technologies); detector: PDA- 100 photodiode array; injector: ASI- 100 autoinjector; pump: p-680A). A flow rate of 1.0 mL/ min was used with mobile phase of MeOH in H_2O with 0.1 % modifier (ammonia v/v).

***Tert*-butyl (3-((5-bromo-2-chloropyrimidin-4-yl)amino)phenyl)carbamate (12a)**

General procedure for the synthesis of **12b**- **12u**. To a solution of 5-bromo-2, 4-dichloropyrimidine (22.79 g, 100 mmol) and *tert*-butyl (3-aminophenyl)carbamate (20.83 g, 100 mmol) in DMF (100 mL), K_2CO_3 (27.64 g, 200 mmol) was added. The suspension was stirred overnight. 200 mL of ice water was added to the reaction mixture and then extracted with dichloromethane (DCM), washed with brine and dried over Na_2SO_4. After filtration, evaporation, the condensation was purified with a silica gel column to yield compound **12a** (39.4 g, 99 %). ^{1}H NMR (400 MHz, DMSO-d_6), δ 9.43 (s, 1 H), 9.28 (s, 1 H), 8.44 (s, 1 H), 7.66 (s, 1 H), 7.25 (d 1 H, *J* = 2.8 Hz), 7.24 (s, 1 H), 7.13 (dd, 1 H, *J* = 2.4, 4.0 Hz), 1.48 (s, 9 H).

***Tert*-butyl (3-(2-chloro-5-methyl-7-oxopyrido[2,3-*d*]pyrimidin-8(7*H*)-yl)-phenyl)carbamate (13a)**

General procedure for the synthesis of **13b- 13u.** Compound **12a** (10.3 g, 25.76 mmol) and trans-crotonic acid (11.08 g, 128.8 mmol) were mixed in dry THF (50 mL) and DIPEA (44.8 mL) under argon. The slurry was stirred, evacuated and refilled with argon before bis(benzonitrile)palladium(II) dichloride (0.494 g, 1.29 mmol) and tri-*o*-tolylphosphine (0.392 g, 1.29 mmol) were added. The mixture was then heated and stirred at 70 °C for 16 hrs and then 6 mL of Ac_2O was added. The reaction mixture was heated and stirred at 90 °C for an additional 24 hrs. The solvent was filtered and then removed under reduced pressure and the residue was diluted with DCM. The organic layer was separated and washed with 1N HCl (3 ×) and brine, dried over anhydrous Na_2SO_4, concentrated and purified by silica gel chromatography to afford compound **13a** (2.235 g, 25 %). ^{1}H NMR (500 MHz, DMSO-d_6), δ 9.56 (s, 1 H), 9.09 (s, 1 H), 7.46-7.38 (m, 3 H), 6.88 (d, 1 H, *J* = 7.5 Hz) 6.71 (d, 1 H, *J* = 1.0 Hz), 2.49 (s, 3 H), 1.46 (s, 9 H).

8-(3-Aminophenyl)-2-((1-(2-(dimethylamino)ethyl)-1*H*-pyrazol-4-yl)amino)-5-methyl-pyrido[2,3-*d*]pyrimidin-7(8*H*)-one (15a)

General procedure for the synthesis of **15b- 15u**. To a solution of compound **13a** (0.41 g, 1.06 mmol) in 2-butanol (5 mL), 1-(2-(dimethylamino)ethyl)-1*H*-pyrazol-4-amine (0.196 g, 1.27 mmol) and trifluoroacetic acid (94 μL) were added in a sealed tube. The reaction was heated at 95 °C for 18 hrs. The reaction mixture was then allowed to cool to room temperature. The mixture was transferred to a round-bottom flask and then the solvent was removed under reduced pressure. The residue was dissolved in DCM (2.0 mL) and TFA (2.0 mL), and the resulting mixture was stirred for 5 hrs at room temperature. The solvent was removed under reduced pressure, and the residue was neutralized with saturated $NaHCO_3$ aqueous solution. The water layer was extracted with DCM. The organic layer was combined and washed with brine, dried over Na_2SO_4, filtered, concentrated, and purified by silica gel chromatography to afford **15a** as a yellow solid (0.264 g, 65 % for two steps). ^{1}H NMR (500 MHz, DMSO-d_6), δ 10.00 (s, 1 H), 8.78 (s, 1 H), 7.25-7.22 (m, 1 H), 7.18 (s, 1 H), 6.95 (s, 1 H), 6.73 (d, 1 H, *J* = 8.0 Hz), 6.44 (s, 1 H), 6.40 (d, 1 H, *J* = 8.0 Hz), 6.26 (s, 1 H), 5.34 (s, 2 H), 3.89 (t, 2 H, *J* = 6.5 Hz), 2.43-2.40 (m, 5 H), 2.16 (s, 6 H).

***N*-(3-(2-((1-(2-(Dimethylamino)ethyl)-1*H*-pyrazol-4-yl)amino)-5-methyl-7-oxopyrido[2,3-*d*]pyrimidin-8(7*H*)-yl)phenyl)acrylamide (9a)**

General procedure for the synthesis of **9a- 9u.** Acryloyl chloride (110 μL) was added dropwise to a mixture of **15a** (264 mg, 0.65 mmol) and DIPEA (0.23 mL) in dry DCM (20 mL) at 0 °C. The

reaction mixture was stirred at 0 ℃ for 30 min and concentrated under reduced pressure. The resulting crude product was purified by silica gel chromatography to afford **9a** as a yellow solid (149 mg, 50 %). ^{1}H NMR (500 MHz, DMSO-d_6) δ 10.40 (s, 1 H), 10.06 (s, 1 H), 8.81 (s, 1 H), 7.86 (d, 1 H, *J* = 8 Hz), 7.65 (s, 1 H), 7.59 (t, 1 H, *J* = 8.0 Hz), 7.13 (s, 1 H), 7.05 (d, 1 H, *J* = 7.6 Hz), 6.77 (s, 1 H), 6.42 (dd, 1 H, *J* = 10.1, 10.1 Hz), 6.30-6.23 (m, 2 H), 5.76 (d, 1 H, *J* = 10.2 Hz), 3.83-3.76 (m, 2 H), 2.46 (s, 3 H), 2.43-2.40 (m, 2 H), 2.09 (s, 6 H). ^{13}C NMR (125 MHz, DMSO-d_6), δ 163.3, 162.2, 157.6, 156.6, 156.5, 147.1, 140.2, 137.6, 131.6, 129.7, 129.1, 127.2, 124.1, 122.2, 119.6, 119.0, 118.9, 116.0, 105.3, 58.7, 49.5, 44.9, 17.0. HRMS (ESI) for $C_{24}H_{26}N_8O_2$ $[M+H]^+$, Calcd: 459.22515, Found: 459.22604, RT= 0.41 min. HPLC analysis: MeOH-H_2O (75: 25), RT= 4.08 min, 98.6 % purity.

***N*-(3-(5-Methyl-2-((1-(1-methylpiperidin-4-yl)-1*H*-pyrazol-4-yl)amino)-7-oxopyrido[2,3-*d*]pyrimidin-8(7*H*)-yl)phenyl)acrylamide (9b)**

^{1}H NMR (400 MHz, DMSO-d_6), δ 10.38 (s, 1 H), 10.04 (s, 1 H), 8.81 (s, 1 H), 7.92 (d, 1 H, *J* = 8.2 Hz), 7.61 (s, 1 H), 7.58 (t, 1 H, *J* = 8.0 Hz), 7.18 (s, 1 H), 7.03 (d, 1 H, *J* = 8.5 Hz), 6.86 (s, 1 H), 6.43 (dd, 1 H, *J* = 10.1, 10.1 Hz), 6.29 (d, 1 H, *J* = 0.9 Hz), 6.25 (dd, 1 H, *J* = 1.9, 2.0 Hz), 5.77 (dd, 1 H, *J* = 1.9, 2.0 Hz), 3.60-3.53 (m, 1 H), 2.84-2.76 (m, 2 H), 2.46 (s, 3 H), 2.22 (s, 3 H), 2.06-1.99 (m, 2 H), 1.80-1.70 (m, 2 H), 1.63-1.55 (m, 2 H). ^{13}C NMR (125 MHz, DMSO-d_6), δ 164.2, 163.1, 158.6, 157.5, 147.9, 141.0, 138.5, 132.5, 130.6, 129.8, 128.1, 125.1, 122.8, 120.6, 120.0, 118.7, 116.9, 106.2, 59.0, 55.0, 54.9, 46.6, 32.8, 17.9. HRMS (ESI) for $C_{26}H_{28}N_8O_2$ $[M+H]^+$, Calcd: 485.2408, Found: 485.24059, RT= 0.41 min. HPLC analysis: MeOH-H_2O (75: 25), RT= 5.68 min, 99.4 % purity.

***N*-(3-(5-methyl-2-((6-(4-methylpiperazin-1-yl)pyridin-3-yl)amino)-7-oxo-pyrido[2,3-*d*]pyrimidin-8(7*H*)-yl)phenyl)acrylamide (9c)**

^{1}H NMR (500 MHz, DMSO-d_6), δ 8.65 (s, 1 H), 8.49 (s, 1 H), 7.82 (br, 2 H), 7.45 (s, 1 H), 7.39 (t, 1 H, *J* = 7.8 Hz), 7.29 (s, 1 H), 7.25 (s, 1 H), 6.88 (d, 1 H, *J* = 7.7 Hz), 6.39 (s, 1 H), 6.33 (d, 1 H, *J* = 16.8 Hz), 6.23 (br, 1 H), 6.12 (dd, 1 H, *J* = 10.2, 10.2 Hz), 5.64 (d, 1 H, *J* = 10.2 Hz), 3.43 (s, 4 H), 2.49-2.48 (m, 7 H), 2.33 (s, 3 H). ^{13}C NMR (125 MHz, DMSO-d_6), δ 163.2, 162.1, 158.5, 156.6, 156.2, 154.8, 146.9, 139.9, 138.3, 137.0, 131.7, 129.5, 128.4, 127.5, 127.1, 123.9, 119.7, 118.9, 116.4, 105.9, 105.7, 54.3, 45.8, 45.1, 16.9. HRMS (ESI) for $C_{27}H_{28}N_8O_2$ $[M+H]^+$, Calcd: 497.2408, Found: 497.24036, RT= 0.3 min. HPLC analysis: MeOH-H_2O (80: 20), RT= 5.63 min,

99.1 % purity.

_N_-(3-(5-Methyl-2-((5-methyl-4,5,6,7-tetrahydrothiazolo[5,4-_c_]pyridin-2-yl)amino)-7-oxopyrido[2,3-_d_]pyrimidin-8(7_H_)-yl)phenyl)acrylamide (9d)

^{1}H NMR (400 MHz, DMSO-d_6), δ 11.74 (s, 1 H), 10.33 (s, 1 H), 8.95 (s, 1 H), 7.82 (d, 1 H, J = 8.3 Hz), 7.64 (s, 1 H), 7.51 (t, 1 H, J = 8.0 Hz), 7.01 (d, 1 H, J = 8.6 Hz), 6.44 (dd, 2 H, J = 10.2, 11.6 Hz), 6.25 (dd, 1 H, J = 1.7, 1.8 Hz), 5.76 (dd, 1 H, J = 1.7, 1.8 Hz), 3.23 (s, 2 H), 2.60 (d, 2 H, J = 5.26 Hz), 2.52 (d, 2 H, J = 6.58 Hz), 2.32 (s, 3 H). ^{13}C NMR (125 MHz, DMSO-d_6), δ 163.18, 162.03, 156.88, 156.01, 155.69, 146.81, 142.44, 140.58, 137.19, 131.69, 129.97, 127.05, 124.3, 120.2, 119.0, 118.7, 117.8, 107.2, 51.9, 50.9, 44.7, 32.9, 31.5, 29.4, 28.9, 25.9, 17.0. HRMS (ESI) for $C_{30}H_{33}N_7O_3$ $[M+H]^+$, Calcd: 474.17067, Found: 474.17037, RT= 0.42 min. HPLC analysis: MeOH-H_2O (85: 15), RT= 5.12 min, 96.7 % purity.

_N_-(3-(2-((4-(3,4-Dimethylpiperazin-1-yl)-2-methoxyphenyl)amino)-5-methyl-7-oxopyrido-[2,3-_d_]pyrimidin-8(7_H_)-yl)phenyl)acrylamide (9e)

^{1}H NMR (400 MHz, DMSO-d_6), δ 10.34 (s, 1 H), 8.79 (s, 1 H), 8.10 (s, 1 H), 7.91 (s, 1 H), 7.53 (s, 1 H), 7.49 (d, 1 H, J = 7.9 Hz), 7.26 (s, 1 H, J = 8.3 Hz), 6.96 (d, 1 H, J = 7.4 Hz), 6.50 (s, 1 H), 6.46-6.39 (m, 1 H), 6.32 (s, 1 H), 6.25 (d 1 H, J = 16.6 Hz), 5.97 (s, 1 H), 5.76 (d, 1 H, J = 9.8 Hz), 3.77 (s, 3 H), 3.39-3.39 (m, 2 H), 2.78 (d, 1 H, J = 10.6 Hz), 2.62 (s, 1 H), 2.53 (s, 1 H), 2.45 (s, 3 H), 2.25 (s, 2 H), 2.20 (s, 3 H), 2.09-2.08 (m, 1 H). ^{13}C NMR (125 MHz, DMSO-d_6), δ 164.1, 163.0, 157.5, 157.2, 147.8, 140.9, 138.0, 132.7, 130.4, 128.0, 124.9, 120.6, 119.6, 117.4, 107.0, 100.4, 58.1, 56.6, 55.9, 49.5, 43.1, 17.9, 17.8. HRMS (ESI) for $C_{30}H_{33}N_7O_3$ $[M+H]^+$, Calcd: 540.27176, Found: 540.27057, RT= 0.41 min. HPLC analysis: MeOH-H_2O (85: 15), RT= 5.12 min, 96.8 % purity.

_N_-(3-(2-((2-Methoxy-4-(3,4,5-trimethylpiperazin-1-yl)phenyl)amino)-5-methyl-7-oxopyrido[2,3-_d_]pyrimidin-8(7_H_)-yl)phenyl)acrylamide（9f）

^{1}H NMR (500 MHz, DMSO-d_6), δ 10.36 (s, 1 H), 8.79 (s, 1 H), 8.12 (s, 1 H), 7.96 (s, 1 H), 7.50 (t, 2 H, J = 7.7 Hz), 7.26 (d, 1 H, J = 8.8 Hz), 6.96 (d, 1 H, J = 7.9 Hz), 6.50 (s, 1 H), 6.46- 6.40 (m, 1 H), 6.32 (s, 1 H), 6.26 (d, 1 H, J = 17.0 Hz), 5.96 (s, 0.7 H), 5.77 (s, 1 H, J = 10.4 Hz), 3.77 (s, 3 H), 2.45 (s, 3 H), 2.25 (s, 4 H), 2.18 (s, 3 H), 1.08 (d, 6 H, J = 4.9 Hz). ^{13}C NMR (125 MHz, DMSO-d_6), δ 164.2, 163.1, 157.5, 157.2, 147.9, 140.9, 138.0, 132.7, 130.5, 128.1, 124.9, 120.6, 119.7, 117.4, 107.1, 106.9, 100.3, 58.2, 56.7, 56.5, 38.4, 18.8, 17.9. HRMS (ESI) for $C_{27}H_{33}N_7O_3$

$[M+H]^+$, Calcd: 554.28741, Found: 554.28756, RT= 0.41 min. HPLC analysis: MeOH-H_2O (80: 20), RT= 11.5 min, 99.9 % purity.

8-((1-Acryloylpyrrolidin-3-yl)methyl)-2-((2-methoxy-4-(4-methylpiperazin-1-yl)phenyl)amino)-5-methylpyrido[2,3-*d*]pyrimidin-7(8*H*)-one (9g)

^{1}H NMR (400 MHz, $CDCl_3$) δ 8.62 (d, 1 H, *J* = 3.76 Hz), 8.16 (dd, 1 H, *J* = 8.44, 8.72 Hz), 7.68 (d, 1 H, *J* = 25.4 Hz), 6.58-6.51 (m, 2 H), 6.40-6.31 (m, 2 H), 6.27 (s, 1 H), 5.65-5.58 (m, 1 H), 4.54-4.35 (m, 2 H), 3.90 (s, 3 H), 3.78-3.58 (m, 2 H), 3.50-3.40 (m, 2 H), 3.19-3.18 (m, 4 H), 2.97-2.85 (m, 1 H), 2.60 (t, 4 H, *J* = 9.8 Hz), 2.40 (s, 3 H), 2.36 (s, 3 H), 2.06-1.85 (m, 2 H). ^{13}C NMR (125 MHz, $CDCl_3$), δ 164.4, 163.4, 159.2, 159.0, 155.8, 155.6, 149.9, 149.5, 148.3, 148.1, 145.3, 128.6, 127.2, 120.9, 120.8, 120.6, 117.2, 107.6, 107.1, 100.2, 55.7, 55.1, 50.3, 49.7, 49.3, 46.0, 45.8, 45.3, 42.4, 42.2, 38.8, 36.0, 29.6, 29.4, 28.5, 17.2. HRMS (ESI) for $C_{28}H_{35}N_7O_3$ $[M+H]^+$, Calcd: 518.28741, Found: 518.28699, RT= 0.42 min. HPLC analysis: MeOH-H_2O (80: 20), RT= 6.81 min, 98.0 % purity.

(*S*)-8-(1-Acryloylpyrrolidin-3-yl)-2-((2-methoxy-4-(4-methylpiperazin-1-yl)phenyl)amino)-5-methylpyrido[2,3-*d*]pyrimidin-7(8*H*)-one (9h)

$[\alpha]_D^{25}$ 25.862 (c 0.015, CH_3OH). ^{1}H NMR (400 MHz, DMSO-d_6), δ 8.73 (s, 1 H), 8.69 (s, 1 H), 7.33 (s, 1 H), 6.55-6.39 (m, 2 H), 6.18-6.12 (m, 2 H), 5.88 (s, 1 H), 5.66 (dd, 1 H, *J* = 11.7, 10.7 Hz), 3.82 (t, 0.7 H, *J* = 9.8 Hz), 3.75 (s, 3 H), 3.67 (s, 0.8 H), 3.59-3.51 (m, 2 H), 3.14-3.12 (m, 5 H), 2.80-2.68 (m, 1 H), 2.55 (s, 4 H), 2.35 (s, 3 H), 2.27 (d, 3 H, *J* = 7.4 Hz), 1.90 (d, 1 H, *J* = 42.9 Hz). ^{13}C NMR (125 MHz, DMSO-d_6), δ 163.1, 163.0, 162.5, 162.4, 159.8, 159.7, 156.9, 156.8, 155.2, 153.1, 152.8, 149.5, 149.4, 146.2, 146.1, 129.5, 128.9, 126.6, 125.3, 125.2, 118.8, 118.6, 115.8, 106.4, 106.3, 99.5, 55.4, 55.2, 54.4, 49.7, 48.3, 48.1, 47.8, 45.5, 45.4, 45.1, 44.7, 43.9, 26.4, 24.5, 16.6. HRMS (ESI) for $C_{27}H_{33}N_7O_3$ $[M+H]^+$, Calcd: 504.27176, Found: 504.27127, RT= 0.42 min. HPLC analysis: MeOH-H_2O (80: 20), RT= 6.87 min, 95.9 % purity.

(*R*)-8-(1-Acryloylpyrrolidin-3-yl)-2-((2-methoxy-4-(4-methylpiperazin-1-yl)phenyl)amino)-5-methylpyrido[2,3-*d*]pyrimidin-7(8*H*)-one (9i)

$[\alpha]_D^{25}$ -39.216 (c -0.020, CH_3OH). ^{1}H NMR (400 MHz, $CDCl_3$), δ 8.76 (d, 2 H, *J* = 17.1 Hz), 7.35 (d, 1H, *J* = 23.1 Hz), 6.59 (s, 1 H), 6.48-6.43 (m, 2 H), 6.16 (dd, 2 H, *J* = 5.8, 9.8 Hz), 5.87 (s, 1 H), 5.69 (dd, 1 H, *J* = 10.1, 10.5 Hz), 4.07 (t, 1 H, *J* = 9.3 Hz), 3.82 (t, 1 H, *J* = 11.0 Hz), 3.76 (d,

3 H, *J* = 6.5 Hz), 3.64 (s, 1 H), 3.55 (d, 2 H, *J* = 10.7 Hz), 3.41 (m, 3 H), 3.13 (m, 4 H), 2.79-2.68 (m, 5 H), 2.36 (s, 3H), 1.91 (dd, 1 H, *J* = 7.2, 4.1 Hz). ^{13}C NMR (125 MHz, $CDCl_3$)), δ 163.2, 163.1, 162.4, 162.3, 159.7, 159.6, 156.8, 156.7, 155.2, 152.9, 152.8, 147.8, 146.0, 145.9, 129.4, 129.0, 126.6, 126.4, 125.2, 124.9, 120.0, 119.7, 116.1, 115.9, 107.0, 106.4, 100.4, 100.3, 55.6, 55.5, 53.2, 52.0, 51.9, 49.7, 48.5, 45.7, 45.4, 44.8, 43.9, 41.9, 41.8, 41.4, 26.6, 24.6, 17.8, 16.6, 16.5, 11.8. HRMS (ESI) for $C_{27}H_{33}N_7O_3$ $[M+H]^+$, Calcd: 504.27176, Found: 504.26978, RT= 0.31 min. HPLC analysis: MeOH-H_2O (80: 20), RT= 5.70 min, 99.6 % purity.

8-(1-Acryloylpiperidin-4-yl)-2-((2-methoxy-4-(4-methylpiperazin-1-yl)phenyl)amino)-5-methylpyrido[2,3-*d*]pyrimidin-7(8*H*)-one (9j)

^{1}H NMR (400 MHz, $CDCl_3$), δ 8.60 (s, 1 H), 8.13 (d, 1 H, *J* = 8.2 Hz), 7.65 (s, 1 H), 6.64 (dd, 1 H, *J* = 10.6, 10.5 Hz), 6.54-6.51 (m, 2 H), 6.32-6.22 (m, 2 H), 5.70 (d, 1 H, *J* = 11.1 Hz), 5.65 (m, 1 H), 4.91 (d, 1 H, *J* = 10.8 Hz), 4.16 (d, 1 H, *J* = 12.4 Hz), 3.90 (s, 3 H), 3.20 (t, 4 H, *J* = 4.5 Hz), 3.02 (s, 2 H), 2.78 (t, 1 H, *J* = 12.5 Hz), 2.60 (t, 4 H, *J* = 4.6 Hz). 2.37 (s, 6 H), 1.76-1.68 (m, 3 H). ^{13}C NMR (125 MHz, DMSO-d_6), δ 164.2, 162.6, 159.3, 156.5, 155.2, 151.8, 148.9, 145.5, 128.5, 126.7, 123.6, 119.1, 116.7, 106.6, 106.3, 99.7, 55.5, 54.5, 50.9, 48.3, 45.6, 16.4. HRMS (ESI) for $C_{28}H_{35}N_7O_3$ $[M+H]^+$, Calcd: 518.28741, Found: 518.28524, RT= 0.32 min. HPLC analysis: MeOH-H_2O (80: 20), RT= 8.33 min, 99.3 % purity.

***N*-(5-(2-((2-Methoxy-4-(4-methylpiperazin-1-yl)phenyl)amino)-5-methyl-7-oxopyrido[2,3-*d*]pyrimidin-8(7*H*)-yl)-2-methylphenyl)acrylamide (9k)**

^{1}H NMR (400 MHz, DMSO-d_6), δ 9.56 (s, 1 H), 8.77 (s, 1 H), 8.08 (s, 1 H), 7.50 (s, 1 H), 7.39 (d, 1 H, *J* = 8 Hz), 7.25 (d, 1 H, *J* = 8.7 Hz), 6.98 (d, 1 H, *J* = 7.5 Hz), 6.61-6.55 (m, 1 H), 6.53 (s, 1 H), 6.29 (s, 1 H), 6.21 (d, 1 H, *J* = 16.6 Hz), 6.01 (s, 1 H), 5.73 (d, 1 H, *J* = 9.7 Hz), 3.77 (s, 3 H), 3.05 (s, 4 H), 2.44 (s, 7 H), 2.36 (s, 3 H), 2.22 (s, 3 H). ^{13}C NMR (125 MHz, DMSO-d_6), δ 163.1, 162.2, 156.4, 156.3, 146.7, 136.9, 134.4, 131.6, 130.8, 130.6, 126.7, 125.6, 123.8, 119.7, 116.4, 106.3, 106.1, 99.6, 55.6, 54.6, 48.6, 45.7, 17.8, 16.9. HRMS (ESI) for $C_{30}H_{33}N_7O_3$ $[M+H]^+$, Calcd: 540.27176, Found: 540.27135, RT= 0.31 min. HPLC analysis: MeOH-H_2O (85: 15), RT= 5.63 min, 97.3 % purity.

***N*-(3-(2-((2-Methoxy-4-(4-methylpiperazin-1-yl)phenyl)amino)-5-methyl-7-oxopyrido[2,3-*d*]pyrimidin-8(7*H*)-yl)-5-methylphenyl)acrylamide (9l)**

^{1}H NMR (400 MHz, DMSO-d_6) δ 10.25 (s, 1 H), 8.79 (s, 1 H), 8.09 (s, 1 H), 7.72 (s, 1 H), 7.36 (s,

1 H), 7.30 (d, 1 H, *J* = 8.9 Hz), 6.80 (s, 1 H), 6.53 (d, 1 H, *J* = 2.0 Hz), 6.43 (dd, 1 H, *J* = 10.0, 10.1 Hz), 6.31 (s, 1 H), 6.24 (dd, 1 H, *J* = 1.6, 1.6 Hz), 6.02 (br, 1 H), 5.75 (d, 1 H, *J* = 11.7 Hz), 3.78 (s, 3 H), 3.03 (s, 4 H), 2.45-2.44 (m, 7 H), 2.34 (s, 3 H), 2.22 (s, 3 H). ^{13}C NMR (125 MHz, DMSO-d_6), δ 163.1, 162.1, 156.4, 156.2, 146.8, 139.7, 138.8, 136.8, 131.7, 126.9, 124.5, 119.8, 119.2, 116.9, 116.5, 106.1, 99.6, 55.7, 54.5, 48.5, 45.7, 21.1, 16.9. HRMS (ESI) for $C_{30}H_{33}N_7O_3$ $[M+H]^+$, Calcd: 540.27176, Found: 540.27197, RT= 0.11 min. HPLC analysis: MeOH-H_2O (80: 20), RT= 10.27 min, 99.7 % purity.

***N*-(3-Ethyl-5-(2-((2-methoxy-4-(4-methylpiperazin-1-yl)phenyl)amino)-5-methyl-7-oxopyrido [2,3-*d*]pyrimidin-8(7*H*)-yl)phenyl)acrylamide (9m)**

^{1}H NMR (500 MHz, DMSO-d_6) δ 10.27 (s, 1 H), 8.79 (s, 1 H), 8.08 (s, 1 H), 7.75 (s, 1 H), 7.38 (s ,1 H), 7.26 (d, 1 H, *J* = 8.9 Hz), 6.83 (s, 1 H), 6.52 (d, 1 H, *J* = 2.4 Hz), 6.42 (dd, 1 H, *J* = 10.1, 10.2 Hz), 6.31 (s, 1 H), 6.24 (dd, 1 H, *J* = 1.9, 2.0 Hz), 5.97 (br, 1 H), 5.75 (dd, 1 H, *J* = 1.8, 1.9 Hz), 3.77 (s, 3 H), 3.02 (s, 4 H), 2.65 (q, 2 H, *J* = 7.5 Hz), 2.45 (s, 3 H), 2.44-2.42 (m, 4 H), 2.22 (s, 3 H), 1.19 (t, 3 H, *J* = 7.5 Hz). ^{13}C NMR (125 MHz, DMSO-d_6), δ 163.1, 162.1, 156.4, 156.3, 146.7, 145.2, 139.8, 136.9, 131.7, 126.9, 123.3, 119.8, 117.9, 117.1, 116.5, 106.1, 106.1, 99.6, 55.6, 54.5, 48.6, 45.7, 28.0, 16.9, 15.1. HRMS (ESI) for $C_{31}H_{35}N_7O_3$ $[M+H]^+$, Calcd: 554.28741, Found: 554.28706, RT= 0.11 min. HPLC analysis: MeOH-H_2O (80: 20), RT= 12.41 min, 96.9 % purity.

***N*-(3-Isopropyl-5-(2-((2-methoxy-4-(4-methylpiperazin-1-yl)phenyl)amino)-5-methyl-7-oxo-p yrido[2,3-*d*]pyrimidin-8(7*H*)-yl)phenyl)acrylamide (9n)**

^{1}H NMR (400 MHz, DMSO-d_6), δ 10.27 (s, 1 H), 8.79 (s, 1 H), 8.06 (s, 1 H), 7.78 (s, 1 H), 7.38 (s, 1 H),7.22 (d, 1 H, *J* = 8.9 Hz), 6.84 (s, 1 H), 6.51 (d, 1 H, *J* = 2.3 Hz), 6.45-6.37 (m, 1 H), 6.31 (s, 1 H), 6.23 (dd, 1 H, *J* = 1.9, 2.0 Hz), 5.59 (s, 0.7 H), 5.74 (dd, 1 H, *J* = 1.9, 2 Hz), 3.77 (s, 3 H), 3.01 (s, 4 H), 2.95-2.88 (m, 1 H), 2.44 (s, 4 H), 2.42 (d, 3 H, *J* = 4.8 Hz), 2.22 (s, 3 H), 1.20 (dd, 6 H, *J* = 4, 4 Hz). ^{13}C NMR (125 MHz, DMSO-d_6), δ 163.1, 162.0, 156.4, 156.3, 149.9, 146.7, 139.8, 137.0, 131.7, 126.8, 121.9, 119.9, 117.1, 116.5, 106.1, 106.0, 99.6, 55.6, 54.5, 48.5, 45.6, 33.3, 23.7, 23.6, 16.9. HRMS (ESI) for $C_{32}H_{37}N_7O_3$ $[M+H]^+$, Calcd: 568.30306, Found: 568.30285, RT= 0.35 min. HPLC analysis: MeOH-H_2O (85: 15), RT= 7.07 min, 98.4 % purity.

***N*-(3-(*Tert*-butyl)-5-(2-((2-methoxy-4-(4-methylpiperazin-1-yl)phenyl)amino)-5-methyl-7-oxo pyrido[2,3-*d*]pyrimidin-8(7*H*)-yl)phenyl)acrylamide (9o)**

^{1}H NMR (400 MHz, DMSO-d_6) δ 10.34 (s, 1 H), 8.86 (s, 1 H), 8.11 (s, 1 H), 7.98 (s, 1 H), 7.51 (s, 1 H), 7.26 (d, 1 H, *J* = 8.7 Hz), 7.04 (s, 1 H), 6.59 (s, 1 H), 6.49 (dd, 1 H, *J* = 10.0, 10.1 Hz), 6.38 (s, 1 H), 6.31 (d, 1 H, *J* = 16.8 Hz), 6.01 (br, 1 H), 5.82 (d, 1 H, *J* = 10.1 Hz), 3.85 (s, 3 H), 3.08 (s, 4 H), 2.52-2.50 (m, 7 H), 2.29 (s, 3 H), 1.34 (s, 9 H). ^{13}C NMR (125 MHz, DMSO-d_6), δ 163.1, 162.1, 158.1, 156.4,156.3, 152.4, 146.7, 139.7, 136.9, 131.9, 131.8, 126.8, 125.4, 120.8, 119.9, 116.8, 116.6, 115.8, 106.2, 106.1, 99.6, 55.7, 54.4, 48.6, 45.7, 34.6, 31.0, 16.9. HRMS (ESI) for $C_{33}H_{39}N_7O_3$ $[M+H]^+$, Calcd: 582.31871 Found: 582.31817, RT= 0.1 min. HPLC analysis: MeOH-H_2O (80: 20), RT= 18.03 min, 94.8 % purity.

***N*-(3-Fluoro-5-(2-((2-methoxy-4-(4-methylpiperazin-1-yl)phenyl)amino)-5-methyl-7-oxopyrido[2,3-*d*]pyrimidin-8(7*H*)-yl)phenyl)acrylamide (9p)**

^{1}H NMR (400 MHz, $CDCl_3$) δ 8.65 (s, 1 H), 8.53 (s, 1 H), 8.02 (s, 1 H), 7.84 (s, 1 H), 7.41 (s, 1 H), 6.84 (s, 1 H), 6.66 (d, 1 H, *J* = 7.4 Hz), 6.41 (d, 1 H, *J* = 8.8 Hz), 6.34 (d, 2 H, *J* = 5.5 Hz), 6.14- 6.08 (m, 2 H), 5.67 (d, 1 H, *J* = 10.3 Hz), 3.12 (s, 3 H), 2.57 (s, 4 H), 2.46 (s, 3 H), 2.35 (s, 3 H). ^{13}C NMR (125 MHz, DMSO-d_6), δ 163.4, 163.18, 162.2 (d, 1 C, *J* = 239.5 Hz), 156.5, 156.1, 146.9, 140.8 (d, 1 C, *J* = 12.6 Hz), 138.3 (d, 1 C, *J* = 12.5 Hz), 131.3, 127.7, 119.5, 116.3, 115.9, 111.3 (d, 1 C, *J* = 23.5 Hz), 106.0, 105.8, 105.6, 99.6, 55.6, 54.5, 48.4, 45.6, 16.9. HRMS (ESI) for $C_{29}H_{30}FN_7O_3$ $[M+H]^+$, Calcd: 544.24669 Found: 544.2458, RT= 0.41 min. HPLC analysis: MeOH-H_2O (75: 25), RT= 11.16 min, 98.9 % purity.

***N*-(3-Chloro-5-(2-((2-methoxy-4-(4-methylpiperazin-1-yl)phenyl)amino)-5-methyl-7-oxopyrido[2,3-*d*]pyrimidin-8(7*H*)-yl)phenyl)acrylamide (9q)**

^{1}H NMR (500 MHz, DMSO-d_6) δ 10.51 (s, 1 H), 8.80 (s, 1 H), 8.22 (s, 1 H), 8.07 (s, 1 H), 7.42 (s, 1 H), 7.27 (d, 1 H, *J* = 8.8 Hz), 7.17 (s, 1 H), 6.52 (s, 1 H), 6.41 (dd, 1 H, *J* = 10.0, 10.1 Hz), 6.31-6.27 (m, 2 H), 6.05 (br, 1 H), 5.81 (d, 1 H, *J* = 11.1 Hz), 3.77 (s, 3 H), 3.03 (s, 4 H), 2.44 (s, 3 H), 2.43 (s, 4 H), 2.22 (s, 3 H). ^{13}C NMR (125 MHz, DMSO-d_6), δ 163.5, 161.8, 156.5, 156.1, 147.0, 140.8, 138.2, 133.3, 131.3, 127.7, 124.0, 119.5, 118.6, 118.3, 116.3, 106.1, 105.9, 99.6, 55.6, 54.5, 48.5, 45.7, 16.9. HRMS (ESI) for $C_{29}H_{30}ClN_7O_3$ $[M+H]^+$, Calcd: 560.21714, Found: 560.21667, RT= 0.1 min. HPLC analysis: MeOH-H_2O (80: 20), RT= 11.89 min, 98.7 % purity.

***N*-(3-Bromo-5-(2-((2-methoxy-4-(4-methylpiperazin-1-yl)phenyl)amino)-5-methyl-7-oxopyrido[2,3-*d*]pyrimidin-8(7*H*)-yl)phenyl)acrylamide (9r)**

^{1}H NMR (400 MHz, DMSO-d_6) δ 10.48 (s, 1 H), 8.80 (s, 1 H), 8.21 (s, 2 H), 7.46 (s, 1 H),

7.29-7.26 (m, 2 H), 6.53 (d, 1 H, *J* = 2.1 Hz), 6.40 (dd, 1 H, *J* = 9.9, 10 Hz), 6.31-6.26 (m, 2 H), 6.09 (br, 1 H), 5.81 (dd, 1 H, *J* = 1.7, 1.9 Hz), 3.77 (s, 3 H), 3.04 (s, 4 H), 2.45-2.43 (m, 7 H), 2.22 (s, 3 H). ^{13}C NMR (125 MHz, DMSO-d_6), δ 163.5, 161.9, 156.5, 156.1, 147.0, 140.9, 138.4, 131.3, 127.7, 126.7, 121.4, 121.1, 119.6, 118.9, 116.3, 106.1, 105.9, 99.7, 69.7, 55.6, 54.5, 48.5, 45.7, 16.9. HRMS (ESI) for $C_{29}H_{30}BrN_7O_3$ $[M+H]^+$, Calcd: 604.16663, Found: 604.16643, RT= 0.1 min. HPLC analysis: MeOH-H_2O (80: 20), RT= 12.32 min, 99.5 % purity.

***N*-(3-(2-((2-Methoxy-4-(4-methylpiperazin-1-yl)phenyl)amino)-5-methyl-7-oxopyrido[2,3-*d*]pyrimidin-8(7*H*)-yl)-5-(trifluoromethyl)phenyl)acrylamide (9s)**

^{1}H NMR (400 MHz, DMSO-d_6), δ 10.65 (s, 1 H), 8.81 (s, 1 H), 8.33 (s, 1 H), 8.23 (s, 1 H), 7.74 (s, 1 H), 7.47 (s, 1 H), 7.13 (d, 1 H, *J* = 8.4 Hz), 6.51 (s, 1 H), 6.42 (dd, 1 H, *J* = 10.2, 9.9 Hz), 6.33 (s, 2 H), 5.93 (s, 0.6 H), 5.83 (d, 1 H, *J* = 9.9 Hz), 3.75 (s, 3 H), 3.00 (s, 4 H), 2.46 (s, 3 H), 2.42 (s, 4 H), 2.21 (s, 3 H). ^{13}C NMR (125 MHz, DMSO-d_6), δ 164.1, 162.4, 157.0, 156.6, 147.6, 141.1, 138.6, 131.7, 130.7 (q, 1 C, *J* = 31.0 Hz), 128.5, 124.2 (q, 1 C, *J* = 271.0 Hz), 123.9, 121.3, 119.9, 116.7, 115.5, 106.6, 106.2, 100.1, 60.2, 56.1, 55.3, 54.9, 48.9, 46.1, 17.4. HRMS (ESI) for $C_{30}H_{30}F_3N_7O_3$ $[M+H]^+$, Calcd: 594.2435, Found: 594.24518, RT= 0.31 min. HPLC analysis: MeOH-H_2O (85: 15), RT= 6.39 min, 95.3 % purity.

***N*-(3-(2-((4-(3,4-Dimethylpiperazin-1-yl)-2-methoxyphenyl)amino)-5-methyl-7-oxopyrido[2,3-*d*]pyrimidin-8(7*H*)-yl)-5-(trifluoromethyl)phenyl)acrylamide (9t)**

^{1}H NMR (400 MHz, $CDCl_3$), δ 9.02 (s, 1 H), 8.66 (s, 1 H), 8.31 (s, 1 H), 7.75 (s, 1 H), 7.53 (s, 1 H), 7.21 (s, 2 H), 6.36 (s, 2 H), 6.33 (s, 1 H), 6.23-6.18 (m, 1 H), 6.05 (s, 1 H), 5.67 (d, 1 H, *J* = 8.2 Hz), 3.81 (s, 3 H), 3.37 (s, 2 H), 3.13 (s, 2 H), 2.78 (s, 1 H), 2.69 (s, 2 H), 2.54 (s, 3 H), 2.48 (s, 3 H), 1.32 (s, 3 H). ^{13}C NMR (125 MHz, DMSO-d_6), δ 163.7, 161.9, 156.5, 156.1, 147.1, 140.8, 138.1, 131.3, 130.2 (q, 1 C, *J* = 32 Hz), 129.8, 127.8, 127.0, 123.5, 123.8 (q, 1 C, *J* = 271 Hz), 120.7, 120.5, 119.9, 116.3, 115.1, 106.2, 105.9, 99.9, 59.7, 57.6, 55.7, 54.0, 53.7, 53.2, 47.1, 16.9. HRMS (ESI) for $C_{31}H_{32}F_3N_7O_3$ $[M+H]^+$, Calcd: 608.25915, Found: 608.25938, RT= 0.41 min. HPLC analysis: MeOH-H_2O (85: 15), RT= 6.63 min, 98.4 % purity.

***N*-(3-(2-((2-Methoxy-4-(3,4,5-trimethylpiperazin-1-yl)phenyl)amino)-5-methyl-7-oxopyrido[2,3-*d*]pyrimidin-8(7*H*)-yl)-5-(trifluoromethyl)phenyl)acrylamide (9u)**

^{1}H NMR (400 MHz, DMSO-d_6), δ 10.66 (s, 1 H), 8.81 (s, 1 H), 8.38 (s, 1 H), 8.23 (s, 1 H), 7.70 (s, 1 H), 7.46 (s, 1 H), 7.14 (d, 1 H, *J* = 8.8 Hz), 6.49 (s, 1 H), 6.45-6.39 (m, 1 H), 6.33 (s, 2 H), 5.85

(s, 0.7 H), 5.83 (d, 1 H, *J* = 10.4 Hz), 3.76 (s, 3 H), 2.46 (s, 3 H), 2.28 (t, 3 H, *J* = 10.7 Hz), 2.24 (s, 3 H), 2.18 (s, 3 H), 1.07 (d, 6 H, *J* = 5.8 Hz). ^{13}C NMR (125 MHz, DMSO-d_6), δ 163.6, 161.9, 156.7, 156.4, 156.1, 147.1, 140.6, 138.1, 131.2, 130.3 (q, 1 C, *J* = 32.0 Hz), 127.9, 123.7 (q, 1 C, *J* = 271.0 Hz), 123.6, 120.8, 119.3, 116.3, 115.0, 106.1, 105.5, 99.4, 56.9, 55.8, 55.7, 55.6, 37.5, 17.8, 16.9. HRMS (ESI) for $C_{32}H_{34}F_3N_7O_3$ $[M+H]^+$, Calcd: 622.2748, Found: 622.27507, RT= 0.41 min. HPLC analysis: MeOH-H_2O (85: 15), RT= 10.36 min, 96.3 % purity.

5.2 Cell lines and reagents

Cell lines H1975 (NSCLC, $EGFR^{L858R/T790M}$) and A431 (NSCLC, $EGFR^{WT}$) were obtained from American Type Culture Collection (ATCC, Rockville, MD). The cells were maintained at 37 °C in 5 % CO_2 incubator in RPMI 1640 (Gibco, Invitrogen) containing 10 % fetal bovine serum (Gibco, Invitrogen) and 1 % penicillin-streptomycin liquid (Gibco, Invitrogen). The EGFR gene of every cell line was sequenced before use. Rociletinib and osimertinib were synthesized in our chemistry laboratory.

5.3 Enzyme-linked immunosorbent assay (ELISA) kinase assay

Poly (Glu, Tyr) 4:1 (Sigma, St. Louis, MO) (20 μg/ mL) was precoated in 96-well ELISA plates as the substrate. The active kinases were incubated with indicated compounds in 1× reaction buffer (50 mmol/ L HEPES pH 7.4, 20 mmol/ L $MgCl_2$, 0.1 mmol/ L $MnCl_2$, 0.2 mmol/ L Na_3VO_4, 1 mmol/ L DTT) containing 5 μmol/ L ATP at 37 °C for 1 h. After incubation, the wells was washed with PBS, and then incubated with anti-phosphotyrosine (PY99) antibody (Santa Cruz, CA) and horseradish peroxidase (HRP)-conjugated secondary antibody in sequence. The wells were visualized using o-phenylenediamine (OPD) and read using a multi-well spectrophotometer (VERSAmax™, Molecular Devices, Sunnyvale, CA, USA) at 492 nm.

5.4 Cell proliferation assays.

NCI-H1975 and A431 cancer cells were maintained in strict accordance with the instruction and established procedures. The cell proliferation assay was evaluated using SRB (Sulforhodamine B) assay treated for 72 hrs with different concentrations of compounds. The data was calculated using Graph Pad Prism version 4.0. The IC_{50} were fitted using a non-linear regression model with a sigmodial dose-response.

5.5 Western blot analysis.

Western blotting was conducted as previously reported. In brief, cells were seeded to six-well

plates and incubated overnight, and then were treated with or without different concentrations of compounds for 4 hrs and then stimulated with or without EGF (100 ng/ mL) for 10 min. Cell samples were then lysed in 1× SDS lysis buffer. Proteins were resolved by SDS-PAGE and transferred onto polyvinylidene difluoride membranes (Millipore), which were blocked with nonfat milk and hybridized with specific primary antibodies. The bands were visualized using an enhanced chemiluminescence reagent (GE Healthcare) after hybridization with a HRP-conjugated secondary antibody.

5.6 Determination of pharmacokinetic parameters in rats.

Male Sprague-Dawley rats (180-300 g) were dosed with the test compounds intravenously (iv) at 5 mg/ kg and by oral gavage (po) at 25 mg/ kg. The compound was dissolved in 5 % DMSO, 40 % PEG400 and Saline. Blood samples (0.2 mL) were then obtained via orbital sinus puncture at 0 min, 5 min, 15 min, 30 min, 1 h, 2 h, 4 h, 6 h, 8 h, 10 h, 16 h, 24 h, time points and collected into heparinized tubes. Blood samples were centrifuged for cell removal, and the plasma was then transferred to a clean vial and subsequently stored at -80 °C prior to analysis. Test sample concentrations were determined by LC-MS/ MS. Pharmacokinetic parameters were calculated using WinNonlin software.

Acknowledgements

We thank National High Technology Research and Development (863) for Young Scientists program (2015AA020906), Guangdong Province (2015A030306042, 2014TQ01R341 and 2015A030312014), Guangzhou City (201508030036 and 201506010086) for their financial support.

Abbreviations

T, threonine; M, methionine; NSCLC, non-small-cell lung cancer; EGFR, epidermal growth factor receptor; L, leucine; R, arginine; E, glutamic acid; A, alanine; MTD, maximum tolerated dose; PK, pharmacokinetics; F, oral bioavailability; DMF, N, N-dimethylformamide; DIPEA, ethyldiisopropylamine; THF, tetrahydrofuran; Ac_2O, acetic anhydride; TFA, trifluoroacetic acid; DCM, dichloromethane; C_{max}, maximum serum concentration; AUC, area under curve; CLz, clearance rate; iv, intravenous administration; po, oral gavage; Erk, extracellular regulated protein kinases; TLC, thin-layer chromatography; UV, ultraviolet; ppm, parts per million; SRB, Sulforhodamine B; ELISA, enzyme-linked immunosorbent assay.

References

[1]. (a) N. E. Hynes, H. A. Lane, ERRB receptor and cancer: the complexity of targeted inhibitors. Nat. Rev. Cancer 5 (2005) 341-354; (b) A. Russo, T. Franchina, G. R. Ricciardi, A. Picone, G. Ferraro, M. Zanghì, G. Toscano, A. Giordano, V. Adamo, A decade of EGFR inhibition in EGFR-mutated non small cell lung cancer (NSCLC): Old successes and future perspectives. Oncotarget 6 (2015), 26814-26825; (c) Z. Song, Y. Ge, C. Wang, S. Huang, X. Shu, K. Liu, Y. Zhou, X. Ma, Challenges and perspectives on the development of small-molecule EGFR inhibitors against T790M-mediated resistance in non-small-cell lung cancer. J. Med. Chem. 59 (2016) 6580-6594.

[2]. (a) A. J. Barker, K. H. Gibson, W. Grundy, A. A. Godfrey, J. J. Barlow, M. P. Healy, J. R. Woodburn, S. E. Ashton, B. J. Curry, L. Scarlett, L. Henthorn, L. Richard, Studies leading to the identification of ZD1839 (Iressa): an orally active, selective epidermal growth factor receptor tyrosine kinase inhibitor targeted to the treatment of cancer. Bioorg. Med. Chem. Lett. 11 (2001) 1911-1914; (b) S. Xin, Y. Zhao, X. Wang, Y. Huang, J. Zhang, Y. Guo, J. Li, H. Li, Y. Ma, L. Chen, Z. Hu, M. Huang, L. Zhang, The dissociation of gefitinib trough concentration and clinical outcome in NSCLC patients with EGFR sensitive mutations. Sci. Rep. 5 (2015) 12675.

[3]. (a) J. D. Moyer, E. G. Barbacci, K. K. Iwata, L. Arnold, B. Boman, A. Cunningham, C. Diorio, J. Doty, M. J. Morin, M. P. Moyer, M. Neveu, V. A. Pollack, L. R. Pustilnik, M. M. Reynolds, D. Sloan, A. Theleman, P. Miller, Induction of apoptosis and cell cycle arrest by CP-358,774, an inhibitor of epidermal growth factor receptor tyrosine kinase. Cancer Res. 57 (1997) 4838-4848. (b) M. H. Cohen, J. R. Johnson, Y. F. Chen, R. Sridhara, R. Pazdur, FDA drug approval summary: erlotinib (Tarceva) tablets. The oncologist 10 (2005), 461-466. (c) J. W. Neal, S. E. Dahlberg, H. A. Wakelee, S. C. Aisner, M. Bowden, Y. Huang, D. P. Carbone, G. J. Gerstner, R. E. G. J.; Lerner, J. L. Rubin, T. K. Owonikoko, P. J. Stella, P. D. Steen, A. A. Khalid, S. S. Ramalingam, Erlotinib, cabozantinib, or erlotinib plus cabozantinib as second-line or third-line treatment of patients with EGFR wild-type advanced non-small-cell lung cancer (ECOG-ACRIN 1512): a randomised, controlled, open-label, multicentre, phase 2 trial. The Lancet Oncology S1470-2045 (2016) 30561-30567.

[4]. D. Li, L. Ambrogio, T. Shimamura, S. Kubo, M. Takahashi, L. R. Chirieac, R. F. Padera, G. L. Shapiro, A. Baum, F. Himmelsbach, W. J. Rettig, M. Meyerson, F. Solca, H. Greulich, K. K. Wong, BIBW2992, an irreversible EGFR/HER2 inhibitor highly effective in preclinical lung cancer models. Oncogene 27 (2008) 4702-4711.

[5]. (a) S. K. Chan, W. J. Gullick, M. E. Hill, Mutations of the epidermal growth factor receptor in non-small cell lung cancer: search and destroy. Eur. J Cancer 42 (2006) 17-23; (b) A. Tartarone, C. Lazzari, R. Lerose, V. Conteduca, G. Improta, A. Zupa, A. Bulotta, M. Aieta, V. Gregorc, Mechanisms of resistance to EGFR tyrosine kinase inhibitors gefitinib/erlotinib and to ALK inhibitor crizotinib. Lung Cancer 81 (2013) 328-336.

[6]. W. Pao, V. A. Miller, K. A. Politi, G. J. Riely, R. Somwar, M. F. Zakowski, M. G. Kris, H. Varmus, Acquired resistance of lung adenocarcinomas to gefitinib or erlotinib is sssociated with a second mutation in the EGFR kinase domain. PLoS Med. 2 (2005) 225-235.

[7]. W. Zhou, D. Ercan, L. Chen, C. H. Yun, D. Li, M. Capelletti, A. B. Cortot, L. Chirieac, R. E. Iacob, R. Padera, J. R. Engen, K. K. Wong, M. J. Eck, N. S. Gray, P. A. Janne, Novel mutant-selective EGFR kinase inhibitors against EGFR T790M. Nature 462 (2009) 1070-1074.

[8]. A. O. Walter, R. Tjin Tham Sjin, H. J. Haringsma, K. Ohashi, J. Sun, K. Lee, A. Dubrovskiy,

M. Labenski, Z. Zhu, Z. Wang, M. Sheets, T. St Martin, R. Karp, D. van Kalken, P. Chaturvedi, D. Niu, M. Nacht, R. C. Petter, W. Westlin, K. Lin, S. Jaw-Tsai, M. Raponi, T. Van Dyke, J. Etter, Z. Weaver, W. Pao, J. Singh, A. D. Simmons, T. C. Harding, A. Allen, Discovery of a mutant-selective covalent inhibitor of EGFR that overcomes T790M-mediated resistance in NSCLC. Cancer Discov. 3 (2013) 1404-1415.

[9]. (a) D. A. Cross, S. E. Ashton, S. Ghiorghiu, C. Eberlein, C. A. Nebhan, P. J. Spitzler, J. P. Orme, M. R. Finlay, R. A. Ward, M. J. Mellor, G. Hughes, A. Rahi, V. N. Jacobs, M. R. Brewer, E. Ichihara, J. Sun, H. Jin, P. Ballard, K. Al-Kadhimi, R. Rowlinson, T. Klinowska, G. H. Richmond, M. Cantarini, D. W. Kim, M. R. Ranson, W. Pao, AZD9291, an irreversible EGFR TKI, overcomes T790M-mediated resistance to EGFR inhibitors in lung cancer. Cancer Discov. 4 (2014) 1046-1061; (b) S. L. Greig, Osimertinib: first global approval. Drugs 76 (2016) 263-273.

[10]. E. S. Kim, Olmutinib: first global approval. Drugs 76 (2016) 1153-1157.

[11]. (a) H. Cheng, S. K. Nair, B. W. Murray, C. Almaden, S. Bailey, S. Baxi, D. Behenna, S. Cho-Schultz, D. Dalvie, D. M. Dinh, M. P. Edwards, J. L. Feng, R. A. Ferre, K. S. Gajiwala, M. D. Hemkens, A. Jackson-Fisher, M. Jalaie, T. O. Johnson, R. S. Kania, S. Kephart, J. Lafontaine, B. Lunney, K. K. C. Liu, Z. Y. Liu, J. Matthews, A. Nagata, S. Niessen, M. A. Ornelas, S. T. M. Orr, M. Pairish, S. Planken, S. J. Ren, D. Richter, K. Ryan, N. Sach, H. Shen, T. Smeal, J. Solowiej, S. Sutton, K. Tran, E. Tseng, W. Vemier, M. Walls, S. W. Wang, S. L. Weinrich, S. B. Xin, H. W. Xu, M. J. Yin, M. Zientek, R. Zhou, J. C. Kath, Discovery of 1-{(3R,4R)-3[({5-Chloro-2-[(1-methyl-1H-pyrazol-4-yl)amino]-7*H*-pyrrolo[2,3-*d*]pyrimidin-4-yl} oxy)methyl]-4-methoxypyrrolidin-1-yl}prop-2-en-1-one (PF-06459988), a potent, WT sparing, irreversible inhibitor of T790M-containing EGFR mutants. J. Med. Chem. 59 (2016) 2005-2024. (b) G. Lelais, R. Epple, T. H. Marsilje, Y. O. Long, M. McNeill, B. Chen, W. Lu, J. Anumolu, S. Badiger, B. Bursulaya, M. DiDonato, R. Fong, J. Juarez, J. Li, M. Manuia, D. E. Mason, P. Gordon, T. Groessl, K. Johnson, Y. Jia, S. Kasibhatla, C. Li, J. Isbell, G. Spraggon, S. Bender, P. Y. Michellys, Discovery of (R,E)-N-(7-Chloro-1-(1-[4-(dimethylamino)but-2-enoyl]azepan-3-yl)-1*H*-benzo[*d*]imidazol-2-yl)-2-methylisonicotinamide (EGF816), a novel, potent, and WT sparing covalent inhibitor of oncogenic (L858R, ex19del) and resistant (T790M) EGFR mutants for the treatment of EGFR mutant non-small-cell lung cancers. J. Med. Chem. 59 (2016) 6671-6689. (c) Y. Hao, X. Wang, T. Zhang, D. Sun, Y. Tong, Y. Xu, H. Chen, L. Tong, L. Zhu, Z. Zhao, Z. Chen, J. Ding, H. Xie, Y. Xu, H. Li, Discovery and structural optimization of N5-substituted 6,7-dioxo-6,7-dihydropteridines as potent and selective epidermal growth factor receptor (EGFR) inhibitors against L858R/T790M resistance mutation. J. Med. Chem. 59 (2016) 7111-7124; (d) J. Han, S. J. Kaspersen, S. Nervik, K. G. Norsett, E. Sundby, B. H. Hoff, Chiral 6-aryl-furo[2,3-*d*]pyrimidin-4-amines as EGFR inhibitors. Eur. J. Med. Chem. 119 (2016) 278-299.

[12]. (a) S. Chang, L. Zhang, S. Xu, J. Luo, X. Lu, Z. Zhang, T. Xu, Y. Liu, Z. Tu, Y. Xu, X. Ren, M. Geng, J. Ding, D. Pei, K. Ding, Design, synthesis, and biological evaluation of novel conformationally constrained inhibitors targeting epidermal growth factor receptor threonine 790-methionine 790 mutant. J Med. Chem. 55 (2012) 2711-2723; (b) S. Xu, T. Xu, L. Zhang, Z. Zhang, J. Luo, Y. Liu, X. Lu, Z. Tu, X. Ren, K. Ding, Design, synthesis, and biological evaluation of 2-oxo-3,4-dihydropyrimido[4,5-*d*]pyrimidinyl derivatives as new irreversible epidermal growth factor receptor inhibitors with improved pharmacokinetic properties. J. Med. Chem. 56 (2013)

8803-8813.

[13].T. Xu, L. Zhang, S. Xu, C. Y. Yang, J. Luo, F. Ding, X. Lu, Y. Liu, Z. Tu, S. Li, D. Pei, Q. Cai, H. Li, X. Ren, S. Wang, K. Ding, Pyrimido[4,5-*d*]pyrimidin-4(1*H*)-one derivatives as selective inhibitors of EGFR threonine790 to methionine790 (T790M) Mutants. Angewandte Chemie 52 (2013) 7564-7568.

[14].T. Xu, T. Peng, X. Ren, L. Zhang, L. Yu, J. Luo, Z. Zhang, Z. Tu, L. Tong, Z. Huang, X. Lu, M. Geng, H. Xie, J. Ding, K. Ding, C5-substituted pyrido[2,3-*d*]pyrimidin-7-ones as highly specific kinase inhibitors targeting the clinical resistance-related EGFR T790M mutant. Med. Chem. Commun. 6 (2015) 1693-1697.

[15].(a) C. Gabriele, E. Carosati, B. De Boeck, K. Ethirajulu, C. Mackie, T. Howe, R. Vianello, MetaSite: understanding metabolism in human cytochromes from the perspective of the chemist. J. Med. Chem. 48 (2005) 6970-6979; (b) H. V. D. Waterbeemd, D. A. Smith, K. Beaumont, D. K. Walker, Property-based design-optimization of drug absorption and pharmacokinetics. J. Med. Chem. 44 (2001) 1313-1333; (c) J. Han, S. Henriksen, K. G. Nørsett, E. Sundby, B. H. Hoff, Balancing potency, metabolic stability and permeability in pyrrolopyrimidine-based EGFR inhibitors Original Research Article, Eur. J Med. Chem. 124 (2016) 58-604.

[16].M. Ishikawa, Y. Hashimoto, Improvement in aqueous solubility in small molecule drug discovery programs by disruption of molecular planarity and symmetry. J. Med. Chem. 54 (2011) 1539-1554.

Captions

Figure 1. Chemical structures of newly reported selective irreversible $EGFR^{T790M}$ inhibitors.

Figure 2. Pharmacokinetic property-based modification of the pyrido[2,3-*d*]pyrimidine-7-ones as selective $EGFR^{T790M}$ inhibitors

Figure 3. A X-ray crystal structure of compound **8** binding with $EGFR^{T790M}$ (PDB ID: 5GMP). (A) The $EGFR^{T790M}$ kinase is shown in a blue ribbon representation. Compound **8** is shown in yellow stick structure. Hydrogen bonds are indicated by black hatched lines to key amino acids. (B) The X-ray crystal structure with interaction surface is shown.

Figure. 4 Compound **9s** potently and selectively inhibits the activation of EGFR signals in H1975 NSCLC cells (A), while less potent in A431 cancer cells (B). Cells were treated with or without compound **9s** and **3** for 4 hrs at indicated concentration, respectively. Cells were then stimulated by 100 ng/ mL EGFR for 10 min and harvested for Western blot analysis.

Table 1 *In vitro* EGFR inhibition and anti-proliferation data of compounds **9a- 9f.**

Table 2 *In vitro* EGFR inhibition and anti-proliferation data of compounds **9g- 9u**

Table 3. Sprague-Dawley rat PK parameters by intravenous and oral administration

Scheme 1. Synthesis of compounds **9a- 9u**.

Optimization of pyrido[2,3-*d*]pyrimidin-7-ones with improved pharmacokinetic properties.

Compound **9s** potently suppressed $EGFR^{L858R/T790M}$ kinase and H1975 cells.

Compound **9s** exhibited moderate plasma exposure and an oral bioavailability value of 16 %.